The *sen1*$^+$ Gene of *Schizosaccharomyces pombe*, a Homologue of Budding Yeast *SEN1*, Encodes an RNA and DNA Helicase†

Hee-Dai Kim,‡ Joonho Choe,‡ and Yeon-Soo Seo*,§

Center for Cell Cycle Control, Samsung Biomedical Research Institute, Sungkyunkwan University School of Medicine, 300 Chunchun-dong, Jangan-gu, Suwon, Kyounggi, 440-746, Korea, and Department of Biological Sciences, Korea Advanced Institute of Science and Technology, 373-1 Kusong-dong, Yusong-gu, Taejon, 305-701, Korea

Received June 25, 1999; Revised Manuscript Received August 9, 1999

ABSTRACT: Two polynucleotide-dependent ATPases, 95 and 181 kDa in size, have been purified to near homogeneity from cell-free extracts of *Schizosaccharomyces pombe*. Despite their size differences, their biochemical properties were strikingly similar. Both enzymes were capable of unwinding RNA and DNA duplexes in keeping with their ability to hydrolyze ATP in the presence of either ribo- or deoxyribopolynucleotide. In addition, they were capable of unwinding DNA/RNA or RNA/DNA hybrid duplexes and translocated in the 5′ to 3′ direction. These results strongly indicate that they are closely related to each other. Determination of the partial amino acid sequence of the 95-kDa enzyme revealed that it is encoded by the *sen1*$^+$ gene, an *S. pombe* homologue of yeast *SEN1*, a protein essential for the processing of small nucleolar RNA, transfer RNA, and ribosomal RNA. The molecular weight of the *S. pombe* Sen1 protein (SpSen1p) predicted from the *sen1*$^+$ open reading frame was 192.5 kDa, suggesting that the 181-kDa enzyme is likely to be a full-length protein, whereas the 95-kDa polypeptide has arisen by proteolysis. In accord with this possibility, polyclonal antibodies specific to the C-terminal region of *sen1*$^+$ cross-reacted with both 95- and 181-kDa polypeptides. We discuss the biochemical activities associated with SpSen1p and their relevance to the apparently divergent functions ascribed to the yeast Sen1 protein in RNA metabolism.

Helicase enzymes have been isolated from a wide variety of sources from bacteria to humans, as well as from bacteriophages and animal viruses. The biochemical properties of a number of DNA helicases have been reviewed extensively (*1*−*6*). Helicases play a variety of critical roles in essential DNA (replication, repair, recombination) and RNA (splicing, transcription, translation) transactions by abolishing the stable helical structure with energy derived from the hydrolysis of NTPs.[1]

Amino acid sequence comparisons have revealed that many DNA and RNA helicases contain distinct conserved motifs (*4*, *7*). The completed *Saccharomyces cerevisiae* genome database (*8*) revealed more than 80 open reading frames (ORFs) with conserved helicase motifs. The presence of such a large number of helicases not only reflects the variety and complexity of DNA and RNA metabolic reactions but also suggests that helicases participate in processes other than those mentioned above. For example, the *PIF1* gene of *S. cerevisiae* is a DNA helicase that plays a role in mitochondrial DNA maintenance (*9*) and telomere length control (*10*). The defective genes in Bloom's and Werner's syndromes also encode DNA helicases (*11*, *12*), which display symptoms characterized by immunodeficiency and premature aging, respectively. RNA helicase A, also known as human RNA/DNA helicase (*13*, *14*), acts as a cellular cofactor for the constitutive transport element of type D retroviruses (*15*) and mediates the association of CBP (Creb-binding protein) with RNA polymerase II to achieve activated transcription (*16*).

We have isolated two enzymes from extracts of *Schizosaccharomyces pombe* that were purified on the basis of their ATPase activity that was stimulated by either poly(U) or M13 sscDNA. Peptide sequence analyses of the purified proteins confirmed that the enzymes were encoded by the *S. pombe* homologue of *SEN1* (*s*plicing *e*ndo*n*uclease), originally reported to be involved in the tRNA splicing pathway in *S. cerevisiae* (*17*, *18*). The removal of introns from precursor tRNAs is mediated by three catalytic enzymes: a site-specific tetrameric endonuclease that catalyzes both 5′ and 3′ cleavages (*18*−*20*), a monomeric tRNA ligase (*21*, *22*), and an NAD-dependent phosphotransferase that removes a 2′-phosphate from the splice junction to produce mature tRNA (*23*). Whereas each of these proteins provides a unique enzymatic activity in the precursor-tRNA splicing pathway,

† This work was supported by a grant from the Samsung Biomedical Research Institute (to Y.-S.S.) and partly by the Korea Science and Engineering Foundation (to J.C.) through the Research Center for Cell Differentiation at Seoul National University.

* To whom correspondence should be addressed: Tel 82-331-299-6440; Fax 82-331-299-6435; E-mail ysseo@smc.samsung.co.kr.

‡ Korea Advanced Institute of Science and Technology.

§ Sungkyunkwan University School of Medicine.

[1] Abbreviations: ss, single-stranded; ds, double-stranded; ssc, single-stranded circular; RFI, replicative form I; bp, base pair(s); nt, nucleotide; SpSen1p, Sen1 protein of *Schizosaccharomyces pombe*; ScSen1p, Sen1 protein of *Saccharomyces cerevisiae*; FPLC, fast performance liquid chromatography; PMSF, phenylmethanesulfonyl fluoride; DTT, dithiothreitol; BSA, bovine serum albumin; TLC, thin-layer chromatography; PAGE, polyacrylamide gel electrophoresis; SDS, sodium dodecyl sulfate; cpm, counts per minute; TCA, trichloroacetic acid; NTP, nucleoside triphosphate; dNTP, deoxyribonucleoside triphosphate.

10.1021/bi991470c CCC: $18.00
Published on Web 10/15/1999

the role played by ScSen1p is not clearly understood at present. A temperature-sensitive mutation in *SEN1* (*sen1-1*) resulted in a significant reduction in endonuclease activity, accompanied by a marked accumulation of precursor tRNA, suggesting that ScSen1p is involved in the endonucleolytic cleavage of precusor tRNA (*17*). Recently, all four genes encoding the tRNA splicing endonuclease subunits [*SEN2*, *SEN15*, *SEN34*, and *SEN54* (*20*)] have been cloned, confirming that the Sen1 protein is not a subunit of the heterotetrameric endonuclease complex (*20*). For this reason, ScSen1p was postulated to act as a positive effector of the tRNA-splicing endonuclease (*18*), although it was not known how the protein participated in this process. The recent cloning of *SEN1* demonstrated that it shares sequence similarity with *UPF1* of *S. cerevisiae* (*18*), which encodes a DNA and RNA helicase (*24*). This finding suggests that SpSen1p is also a DNA and RNA helicase.

The initial speculation that Sen1 is involved solely in tRNA processing has been obscured by several other findings that suggest more diverse functions for Sen1 in nucleolar RNA-mediated processing and mRNA transcription. For example, (i) a point mutation in the *SEN1* gene resulted in the mislocalization of two nucleolar proteins (Nop1 and Ssb1) to the nucleoplasm (*25-27*); (ii) ScSen1p acts in the transcriptional repression of a chimeric gene that contains an exogenous sequence element, indicating a potential role for ScSen1p in mRNA transcription (*28*); (iii) a mutation in the helicase domain of *SEN1* resulted in the alteration of the cellular abundance of many RNA species, including tRNAs, rRNAs, and small nuclear and nucleolar RNAs (*29*); and (iv) an allele of *SEN1* (named *cik3-1*) was identified in a screen for mutations that cause chromosomal instability (*30*). Most recently, it was shown that the Sen1 protein is required for the maturation and stability of termini of small nucleolar RNAs in *S. cerevisiae* (*31*).

In this report, we present evidence that the *S. pombe* homologue of yeast Sen1 is a DNA- and RNA-dependent ATPase, which possesses both DNA and RNA unwinding activities. On the basis of our findings, we discuss the biochemical activities of SpSen1p and their relevance to a possible role(s) of the enzyme in RNA processing.

EXPERIMENTAL PROCEDURES

Enzymes, Radioisotopes, Polynucleotides, and Plasmids. Radioisotopes that include [γ-^{32}P]ATP, [α-^{32}P]dCTP, [α-^{32}P]-GTP, and [α-^{32}P]UTP (3000 Ci/mmol each) were purchased from Amersham. NTPs and dNTPs were obtained from Boehringer Mannheim. T3, T7, and SP6 RNA polymerases, Klenow fragment of the *Escherichia coli* DNA polymerase I, RNase-free DNase I, RNasin, and T4 polynucleotide kinase were obtained from Promega. All restriction endonucleases were purchased from New England Biolabs. Poly(ethylenimine)−(PEI−) cellulose plates were from J. T. Baker. M13 sscDNA and RFI DNA were purified as described (*32*). Poly-(U), poly(C), poly(A), poly(G), poly(dT), and poly(dA) were obtained from Pharmacia. Yeast tRNAs were from Sigma. Plasmids used to obtain runoff transcripts are pSP65 and pGEM1 (Promega) and pBlueScriptII-SK (Strategene).

Oligonucleotides. Five DNA oligonucleotides (20-, 27-, 28-, 40-, and 98-mers) were commercially synthesized by BioServe Biotechnologies (Laurel, MD) and electrophoretically purified prior to use (*33*). The sequences of the oligonucleotides were as follows: 20-mer, 5′-CTG CAG CCC AAG CTT GTA TT-3′; 27-mer, 5′-CTG GCT TAT CGA AAT TAA TAC GAC TCA-3′; 28-mer, 5′-GAA TAC ACG GAA TTC GAG CTC GCC CGG G-3′; 40-mer, 5′-GAA TAC ACG GAA TTC GAG CTC GCC CGG GGA TCC TCT AGA G-3′; 98-mer, 5′-GAA TAC AAG CTT GGG CTG CAG GTC GAC TCT AGA GGA TCC CCG GGC GAG CTC GAA TTC CGG TCT CCC TAT AGT GAG TCG TAT TAA TTT CGA TAA GCC AG-3′. Two DNA oligonucleotides, the 20-mer and 27-mer, contained sequences complementary to 5′- and 3′-end regions of the 98-mer, respectively, and were used to prepare 5′- and 3′-tailed partial duplex DNA substrates (Figure 1). The 28-mer and 40-mer oligonucleotides have sequences complementary to the central region of the 98-mer as shown in Figure 1.

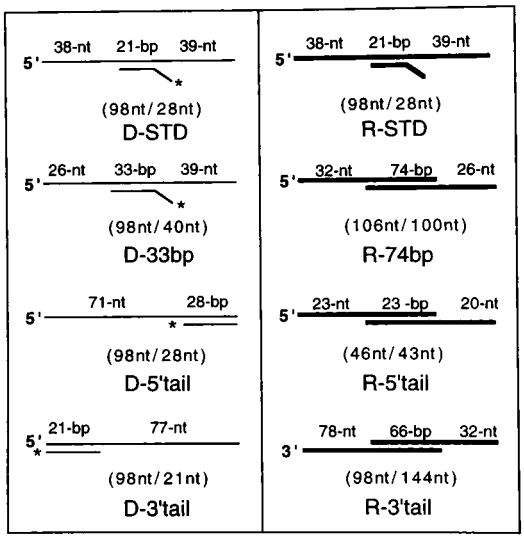

FIGURE 1: Structures and designations of RNA and DNA substrates used to characterize the unwinding activities of the purified SpSen1p. Substrates were prepared as described under Experimental Procedures. RNA strands are depicted by thick lines and DNA strands by thin lines. The sizes of single-stranded and double-stranded regions in each substrate are indicated in nucleotides (nt) and base pairs (bp), respectively. Lengths of RNA transcripts or DNA oligonucleotides used to prepare substrates are noted in parentheses. The names of each substrate are as indicated at the bottom of the schematic diagrams of each substrate: R-STD, standard RNA substrate; D-STD, standard DNA substrate; R-74bp, RNA substrate with 74-bp duplex; D-33bp, DNA substrate with 33-bp duplex; R-5′tail, RNA substrate with 5′-ssRNA overhang; D-5′tail, DNA substrate with 5′-ssDNA overhang; R-3′tail, RNA substrate with 3′-ssRNA overhang; D-3′tail, DNA substrate with 3′-ssDNA overhang. Shorter strands in each RNA substrate had higher (>100-fold) specific activity than did the longer ones (except for R-5′tail). Asterisks indicate the ^{32}P-labeled end of DNA substrates.

Preparation of DNA Helicase Substrates. The structures of each DNA and RNA substrate used in this study are illustrated schematically in Figure 1. The standard DNA substrate (referred to as D-STD, Figure 1) was made by annealing 5′-^{32}P-labeled 28-mer to the unlabeled 98-mer. With this and all the other substrates shown in Figure 1, the unlabeled longer strands serve preferentially as a template to which the enzyme is bound and translocates during unwinding reaction, while the labeled shorter strand is

expected to be displaced by the enzyme. The 28-mer (5 pmol) was first labeled at the 5′-end with [γ-^{32}P]ATP and T4 polynucleotide kinase as recommended by the manufacturer and combined with unlabeled 28-mer oligonucleotide (20 pmol) to obtain specific activities (300−500 cpm/fmol) comparable to that of the RNA standard substrate (see below). The 28-mer pool (25 pmol) was mixed with 20 pmol of the 98-mer in the presence of 50 mM Tris-HCl (pH 7.8), 0.6 M NaCl, and 1 mM EDTA. The mixture (50 μL) was incubated at 95 °C for 5 min, followed by a 30-min incubation at 65 °C, and then cooled slowly to 25 °C at the rate of −0.1 °C/min in a polymerase chain reaction thermocycler (MJ Research). The annealed substrates were purified by electrophoresis on a 10% polyacrylamide gel in 1× TBE [89 mM Tris base, 89 mM boric acid, and 2 mM EDTA]. The recovery (60−80%) and specific activity (300−500 cpm/fmol) of the substrate preparations were calculated on the basis of TCA-precipitable counts present before and after gel purification. The 33-bp duplex (D-33bp, Figure 1) DNA substrate was prepared in a manner similar to D-STD except that the 5′-^{32}P-labeled 40-mer was not diluted with unlabeled oligonucleotide. Therefore, this substrate had a higher specific activity (1500−2500 cpm/fmol) than did D-STD.

The D-3′tail and D-5′tail substrates (Figure 1) were prepared by first hybridizing the 20-mer and 27-mer (20 pmol each), respectively, to the 98-mer (5 pmol) by the same procedure as described above. Then the annealed DNA (3 pmol with respect to the 98-mer) was labeled at the 3′-ends of the 20-mer and 27-mer in a reaction mixture (100 μL) containing [α-^{32}P]dCTP (3.3 pmol) and Klenow fragment (5 units) in 50 mM Tris-HCl (pH 7.2), 10 mM $MgSO_4$, and 0.1 mM DTT (incubation was at 23 °C for 20 min). The reaction was supplemented with excessive cold dCTP (200 μM), incubated for an additional 10 min to ensure complete incorporation of dCMP residues at the 3′ ends, terminated by the addition of EDTA to 10 mM, and filtered through a 1.0-mL Sepharose CL-4B (Pharmacia) column equilibrated with TE buffer [10 mM Tris-HCl (pH 8.0) and 1 mM EDTA]. The pass-through fractions (50 μL) were collected in a 1.5-mL Eppendorf tube. Fractions of the pass-through that were labeled were pooled, and the yield (>80%) was calculated by measuring the radioactivity of TCA-insoluble materials present before and after filtration. The specific activities of DNA substrates in this manner prepared were in the range of 2000−3000 cpm/fmol.

Preparation of RNA Helicase Substrates. All RNA templates were made by in vitro runoff transcription with a combination of RNA polymerase (5 units each) and an appropriate linearized plasmid (5 μg each) in reaction mixtures (50 μL) under conditions recommended by the manufacturer. For each transcript, its size, RNA polymerase, and the restricted vector used are described below and indicated in parentheses: The standard RNA substrate (R-STD, Figure 1) was prepared by annealing two RNA transcripts (28 nt, SP6 RNA polymerase, *Bam*HI-digested pSP65; and 98 nt, SP6 RNA polymerase, *Pvu*II-digested pGEM1). The R-5′tail substrate consisted of two RNA templates (46 nt, SP6 RNA polymerase, *Sac*I-digested pGEM1; and 43 nt, SP6 RNA polymerase, *Acc*I-digested pSP65). The R-3′tail substrate was prepared from two RNA transcripts (98 nt, SP6 RNA polymerase, *Pvu*II-digested pGEM1; and 144 nt, T7 RNA polymerase, *Rsa*I-digested pGEM1). The R-74bp substrate was prepared by hybridizing two transcripts (100 nt, T7 RNA polymerase, *Not*I-cut pBlueScript II-SK; and 106 nt, T3 RNA polymerase, *Xho*I-cut pBlueScriptII-SK). All templates described above were radiolabeled with either [α-^{32}P]UTP or [α-^{32}P]GTP, but the shorter strands had 100-fold higher specific activities (300−500 cpm/fmol) than those of the longer strands (3.0−5.0 cpm/fmol). DNA templates were removed by digestion with RNase-free DNase I following the transcription reactions, and the transcripts were then electrophoretically purified as described above. The subsequent procedures such as annealing and isolation of duplex RNAs were essentially the same as described (*13*). Final preparations of the partial duplex RNAs were also gel-purified, and the yield (20−30%) was determined. The RNA substrates thus obtained were diluted to a concentration of 80 fmol/μL. Their specific activities ranged from 300 to 500 cpm/fmol.

ATPase Assay. The ATPase assay was carried out in a standard reaction mixture (20 μL) containing 20 mM HEPES-KOH (pH 7.8), 50 mM NaCl, 1 mM $MgCl_2$, 2 mM DTT, 100 μg/mL BSA, 0.5−1.0 mM ATP, 0.2 μM [γ-^{32}P]-ATP, and 50 ng of polynucleotides as indicated, and the enzyme fraction. After incubation at 37 °C for 30 min, an aliquot (2 μL) was spotted onto a PEI−cellulose TLC plate. The plates were developed in a solution containing 0.5 M LiCl/1.0 M formic acid and subsequently dried. The hydrolyzed products were analyzed and quantitated with a PhosphorImager (Molecular Dynamics).

Helicase Assay. The unwinding of duplex RNA and DNA substrates was measured in standard reaction mixtures (20 μL) containing 20 mM HEPES-KOH (pH 7.8), 50 mM NaCl, 2 mM ATP, 1 mM $MgCl_2$, 2 mM DTT, 100 μg/mL BSA, 2−5 units of RNasin (omitted in the DNA unwinding reaction), 40 fmol of ^{32}P-labeled partial duplex substrate, and the enzyme fraction. After incubation at 37 °C for 1 h, reactions were terminated with 4 μL of 6× gel-loading buffer [60 mM EDTA (pH 8.0), 40% (w/v) sucrose, 0.6% SDS, 0.25% bromophenol blue, and 0.25% xylene cyanol]. The reaction products were subjected to electrophoresis at 150 V for 60 min through 10% polyacrylamide (29:1) gels containing 0.1% SDS in 1× TBE. The gels were dried and analyzed with a PhosphorImager for quantitation.

Electrophoresis Mobility Shift Assay. The complexes formed between SpSen1p and ssDNA or ssRNA were analyzed in the helicase reaction mixture, except that ssRNA (transcript of *Pvu*II-cut pGEM1, SP6 RNA polymerase, 98-mer) or 5′-labeled ssDNA (98-mer) was added in place of the duplex substrates. The ssRNA and ssDNA were identical in their sequences and sizes. After a 30-min incubation at 37 °C, the reaction mixtures were supplemented with 0.2% glutaraldehyde and 10% glycerol, incubated for 10 min further on ice, and electrophoresed at 100 V through a 6% polyacrylamide gel in 0.5× TBE. The gel was dried and analyzed with a PhosphorImager for quantitation.

Purification of the S. pombe Helicase. The wild-type fission yeast *S. pombe* (strain 972) was grown and extracts were prepared as described previously (*34*). All purification steps were carried out at 4 °C. During the first three steps of the procedure (Table 1), ATP hydrolysis was monitored in the presence and in the absence of polynucleotide cofactors, M13 sscDNA and poly(U). In subsequent purifica-

Table 1: Purification of the 95- and 181-kDa Enzymes from *S. pombe* Extracts

fractions	volume (mL)	protein (mg/mL)	total protein (mg)	total activity[a] (ATP hydrolyzed, μmol)	specific activity (μmol/mg)
			95-kDa		
crude extracts	1634	5.65	9235.6	ND[b]	ND
heparin−Sepharose	340	0.54	181.8	680.5	3.7
DEAE/SP−Sepharose	20	0.64	12.8	128.0	10.0
ssDNA−cellulose	5	0.020	0.098	42.1	430.0
ATP−agarose	0.4	0.030	0.012	7.0	576.0
			181-kDa		
crude extracts	1600	4.66	7460.0	ND[b]	ND
heparin−Sepharose	325	1.39	452.2	723.0	1.6
DEAE−Sepharose	75	1.23	92.3	92.0	1.0
ssDNA−cellulose	5.0	0.46	2.30	32.0	14.0
ATP−agarose	14.0	0.11	1.53	8.2	5.34
Resource S	1.4	0.019	0.026	5.2	199

[a] The standard reactions were carried out in the presence of 50 ng of poly(U) cofactor, as described under Experimental Procedures. [b] ND, not determined.

tion steps, both ATPase and DNA helicase assays were used to monitor active fractions.

Purification of the 95-kDa Enzyme. The extracts (5.65 mg/mL; 1634 mL) prepared as described above were applied first to a heparin−Sepharose (Pharmacia) column (2.5 × 30 cm, 150 mL) equilibrated with buffer T [25 mM Tris-HCl (pH 7.5), 1 mM EDTA, 10% glycerol, 1 mM DTT, 0.1 mM PMSF, 1 mM benzamidine, 0.1 μg/mL pepstatin A, and 0.15 μg/mL leupeptin and antipain] containing 50 mM NaCl. The column was washed with the same buffer, and the protein was eluted with a 2.4-L linear gradient of 50−700 mM NaCl in buffer T. Fractions containing both M13 sscDNA and poly(U)-stimulated ATPase activities eluting at 200 mM NaCl were pooled, dialyzed for 3 h against buffer T (4 L), and adjusted to 50 mM NaCl. The dialyzate (0.54 mg/mL, 340 mL) was loaded onto a double-tandem column that consisted of DEAE-Sepharose (Pharmacia) (top, 2.5 × 8.2 cm, 40 mL) and SP-Sepharose (Pharmacia) (bottom, 1.5 × 8.5 cm, 15 mL) equilibrated with buffer T plus 50 mM NaCl. The top column (DEAE-Sepharose) acted as a negative column that bound the majority of the protein (>80%) without binding the desired one, whereas the bottom column (SP-Sepharose) acted as a positive column that retained the desired protein. After a wash with 400 mL of the same buffer, the SP−Sepharose column was separated and the protein was eluted with a 130-mL linear gradient of 50−400 mM NaCl in buffer T. Fractions containing the ATPase activity, which peaked at 150 mM NaCl, were pooled (0.64 mg/mL, 20 mL) and dialyzed for 6 h against buffer T plus 50 mM NaCl (2 L). The dialyzed protein was loaded onto a ssDNA−cellulose (Sigma) column (0.7 × 3.0 cm, 1.2 mL) equilibrated with buffer T containing 50 mM NaCl at a rate of 2 mL/h. After the column was washed with T buffer containing 50 mM NaCl (15 mL), the protein was eluted with a 20-mL linear gradient of 50−600 mM NaCl in T buffer. Fractions containing ATPase activity, which eluted at 250 mM NaCl, were pooled (0.020 mg/mL, 5.0 mL), diluted to 50 mM NaCl, and loaded onto an ATP−agarose (Sigma A6888) column (0.7 × 3.0 cm, 1.2 mL) equilibrated with buffer T plus 50 mM NaCl. The column was washed with buffer T containing 80 mM NaCl (10 mL), and the protein was eluted with 10 mL of buffer T plus 50 mM NaCl and 2 mM ATP. Fractions from the ATP−agarose column were examined for ATPase activity and silver-stained polypeptides on SDS−PAGE. The fractions (30.3 μg/mL, 0.4 mL) with fewer polypeptides were pooled to obtain those of highest purity at this step. One half of the pooled fractions was diluted 10-fold with storage buffer [buffer T with 50% glycerol and 0.1 mg/mL BSA] and concentrated 10-fold on a Biomax-10k filter (Ultrafree centrifugal filter, Millipore) as recommended by the manufacturer. This treatment was repeated two more times to remove ATP present in the fraction, which interfered with ATPase activity analysis. The resulting preparation was stored at −80 °C. Unless otherwise stated, this fraction was used to examine the helicase and ATPase activities associated with the enzyme. The remaining half of the pooled fractions (6.0 μg, 0.2 mL) was applied directly to a glycerol gradient (5 mL, 15−35% glycerol in buffer T plus 500 mM NaCl) and centrifuged for 24 h at 45 000 rpm in a Beckman SW55 Ti rotor for further analysis. Fractions (220 μL) were collected from the bottom of the gradient and assayed for DNA and RNA helicase and ATPase activities and were subjected to SDS−PAGE.

Purification of the 181-kDa Enzyme. The heparin−Sepharose fraction (1.39 mg/mL, 325 mL) was prepared as described above and loaded onto a DEAE-Sepharose (Pharmacia) column (2.5 × 8.2 cm, 40 mL) equilibrated with buffer T plus 50 mM NaCl. After the column was washed with 400 mL of the same buffer, proteins were eluted with a 400-mL linear gradient of 50−400 mM NaCl in buffer T. ATPase activity, stimulated by both poly(U) and M13 sscDNA, peaked at 150 mM NaCl; these fractions were pooled (1.23 mg/mL, 75 mL) and dialyzed for 3 h against buffer T plus 50 mM NaCl (2 L). The dialyzed protein was loaded at a rate of 3 mL/h onto a ssDNA−cellulose (Sigma) column (1.0 × 2.0 cm, 1.58 mL) equilibrated with buffer T containing 50 mM NaCl. The column was washed with buffer T containing 50 mM NaCl (15 mL), and the protein was eluted with a 30-mL linear gradient of 50−600 mM NaCl in buffer T. Fractions containing ATPase activity, which eluted at 230 mM NaCl, were pooled and dialyzed for 3 h against buffer T plus 50 mM NaCl (2 L). The dialyzed sample (0.46 mg/mL, 5.0 mL) was passed through an ATP−agarose (Sigma A6888) column (0.7 × 3.0 cm, 1.2 mL) equilibrated with buffer T plus 50 mM NaCl, and the column was washed with buffer T containing 80 mM NaCl (10 mL).

The flowthrough and wash fractions were combined (0.11 mg/mL, 14.0 mL), adjusted to 50 mM NaCl with buffer T, and loaded onto an FPLC Resource S (1.0 mL, Pharmacia) column equilibrated with buffer T plus 50 mM NaCl. The column was washed with buffer T containing 50 mM NaCl, and the protein was eluted with a 25-mL linear gradient of 50−400 mM NaCl in buffer T. Fractions from the FPLC Resource S column were examined for ATPase and RNA/DNA helicase activities, and proteins were analyzed by SDS−PAGE and silver staining. The fraction (0.019 mg/mL, 1.4 mL) with fewer polypeptides was selected to obtain those with the highest purity at this stage of the purification. The pooled fraction was concentrated 6-fold on a Biomax-10k filter and was subjected to glycerol gradient sedimentation analysis as described above for the 95-kDa protein.

RESULTS

Purification of the 95-kDa Enzyme. The initial heparin−Sepharose step led to the enrichment of an ATPase(s) that was stimulated by poly(U). Most of the poly(U)-dependent ATPase activity was bound to and eluted from the heparin−Sepharose column and was also stimulated by M13 sscDNA. In contrast, ATPase activities detected in the flowthrough fractions were not stimulated by any polynucleotide (data not shown). Chromatography through a DEAE-Sepharose column resolved two major ATPase activities (the flowthrough and bound fractions) that were stimulated by M13 sscDNA and poly(U). From our previous studies, the fraction bound contains DNA helicase I as a major interfering activity, which is a potent DNA-dependent ATPase (30−50 ATP s^{-1} $enzyme^{-1}$) (*34*). Since DNA helicase I is unable to utilize poly(U) as an effector for ATP hydrolysis (*34*), the bound fraction most likely contains several other ATPases in addition to DNA helicase I. Therefore, we decided to further purify the ATPase activity present in the flowthrough fraction, which is likely to include a new helicase(s) and is free of contamination with DNA helicase I.

For this purpose, we loaded the active heparin−Sepharose fraction onto a double-tandem column that consisted of DEAE-Sepharose (top) and SP-Sepharose (bottom) columns as described under Experimental Procedures. After loading and washing, the two columns were separated and protein was eluted from the bottom SP-Sepharose column with a linear salt gradient. Assays of these fractions indicated that the poly(U)-stimulated ATPase activity still copurified with an M13 sscDNA-stimulated ATPase activity (data not shown), suggesting that a single protein was responsible for both RNA- and DNA-dependent ATPase activities. Major purification (>40-fold) was achieved with the ssDNA−cellulose chromatographic step, which removed more than 99% of contaminating proteins (Table 1). The ATP−agarose column step removed several major contaminating polypeptides present in the ssDNA cellulose fractions and enriched a 95-kDa polypeptide that eluted with 2 mM ATP in a buffer containing 50 mM NaCl (data not shown). The 95-kDa protein was not eluted from the ATP−agarose column with buffers lacking ATP even at higher ionic strength (80 mM) (data not shown), indicating that this column acted as an affinity step. The 95-kDa polypeptide was the only protein that copurified with both ATPase and helicase activities (data not shown). To confirm this observation, we carried out glycerol gradient sedimentation analysis on the ATP−agarose fractions (Figure 2). The ATPase−helicase activity sedimented between aldolase (158 kDa) and BSA (66 kDa) with a sedimentation coefficient of 5.2 S (Figure 2A,B), suggesting that it exists as a monomer of about 95 kDa. Both poly(U)- and M13 sscDNA-dependent ATPase activities were detected coincidentally with the position of the 95-kDa protein (Figure 2A,B). Because the ATPase activity of the purified protein was stimulated by both ssRNA and ssDNA, we investigated whether the enzyme fraction was capable of unwinding dsDNA and dsRNA. By use of the standard DNA (D-STD) and RNA (R-STD) substrates described in Figure 1, the enzyme fraction was found to contain both DNA (Figure 2C) and RNA (Figure 2D) helicase activities, in keeping with the properties of its ATPase activities. Again, the helicase activities cosedimented with the 95-kDa polypeptide, indicating that this protein intrinsically containes all of the observed activities (DNA- and RNA-dependent ATPase and RNA and DNA unwinding activities).

Purification of the 181-kDa Enzyme. Using the chromatographic steps shown in Table 1, we purified another ATPase activity that was also stimulated by either poly(U) or M13sscDNA. The heparin−Sepharose fraction, prepared as described for the 95-kDa enzyme, was loaded onto a DEAE-Sepharose column, which was eluted with a linear NaCl gradient. An activity was detected that peaked at 150 mM NaCl. The specific activity of this fraction was lower than observed with the heparin−Sepharose fraction (Table 1), probably due to removal of the 95-kDa enzyme in the flowthrough fractions, as described above. The ssDNA−cellulose column was effective in removing substantial amounts of contaminating proteins (14-fold purification) (Table 1). When the ssDNA−cellulose fraction was passed through an ATP−agarose column, the activity was not retained by the column, unlike the 95-kDa enzyme (data not shown). This observation suggests that the N-terminal region of the enzyme may negatively affect its ability to form a stable complex with ATP. Noteworthy was that the combined flowthrough and wash fractions decreased (∼3-fold) in specific activity, implying that the enzyme activity was not stable at low protein concentrations (Table 1). Although this procedure resulted in a decrease of specific activity and stability of the desired enzyme, the use of an ATP−agarose column at this stage was essential to remove completely the residual 95-kDa enzyme present in the ssDNA−cellulose fractions. Further purification was achieved with the FPLC Resource S column (Table 1). Both ATPase and RNA/DNA helicase activities comigrated with a 181-kDa polypeptide. Active fractions were pooled, concentrated, and subjected to glycerol gradient sedimentation analysis as described above for the 95-kDa enzyme. As shown in Figure 3, the same 181-kDa polypeptide (Figure 3A) cosedimented with a single peak of RNA/DNA-dependent ATPase (Figure 3B) and DNA and RNA helicase activities (Figure 3, panels C and D, respectively) that possessed a sedimentation coefficient of 8.5 (Figure 3B).

The Purified Enzyme Is Encoded by the SEN1 Homologue of S. cerevisiae. The purified 95-kDa enzyme (50 pmol) was resolved by SDS−PAGE (8%) and transferred to a Nytran cellulose membrane. The band was excised from the membrane and digested with trypsin. Two tryptic peptides yielded the amino acid sequences IGNPETINVSVR and LFDVR (Figure 4) that were uniquely found in the open

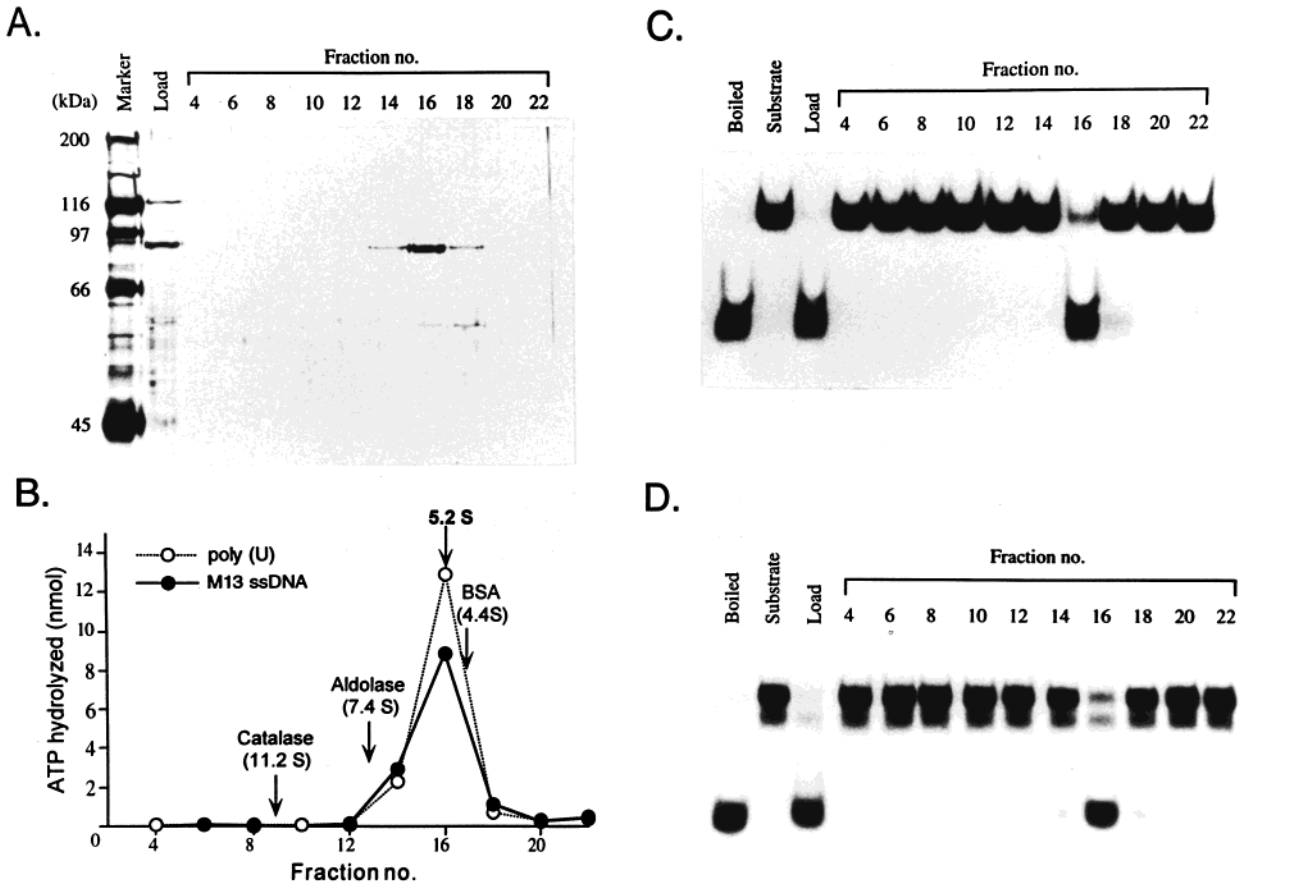

FIGURE 2: Glycerol gradient sedimentation analysis of the 95-kDa enzyme obtained after ATP−agarose chromatography. The active fractions (15 μg, 0.2 mL) from the ATP−agarose column were loaded onto a 15−35% glycerol gradient and centrifuged as described under Experimental Procedures. Fractions (0.22 mL) were collected from the bottom of the tube. Proteins were analyzed on an SDS−8% polyacrylamide gel, and ssRNA- and ssDNA-dependent ATPase and RNA/DNA helicase activities were assayed across the glycerol gradient fractions. (A) Silver-stained protein gel of the glycerol gradient fractions (20 μL). The load (pooled fractions from the ATP−agarose step) and glycerol gradient fractions analyzed are indicated at the top of the figure. The following protein markers (Bio-Rad) were used: myosin (200 kDa), β-galactosidase (116 kDa), phosphorylase B (97 kDa), BSA (66 kDa), and ovalbumin (45 kDa). The sedimentation value of the helicase (5.2 S) was determined with reference to marker proteins, which included BSA (4.4 S), aldolase (7.4 S), and catalase (11.2 S) run in a parallel gradient. The sedimentation profile of the marker proteins was determined with the use of the Bradford protein assay (*50*). (B) M13 sscDNA-dependent (●) and poly(U)-dependent (○) ATPase activities were measured. The ATPase activity was assayed with 2 μL of each glycerol gradient fraction in 20-μL reactions in the presence of 1.5 mM ATP as described under Experimental Procedures. (C, D) Autoradiograms of the DNA (panel C) and RNA helicase (panel D) reactions are shown. DNA and RNA helicase activities were measured in reaction mixtures (20 μL) that contained 2 μL of each glycerol gradient fraction with 20 fmol of D-STD and R-STD substrates under the conditions described in Experimental Procedures. The reaction products were resolved by electrophoresis through a 10% nondenaturing polyacrylamide gel. The boiled substrate, substrate-only, and load controls are indicated above the appropriate lanes.

reading frame (GenBank accession no. Z81317) on cosmid C6G9.10C containing S. *pombe* chromosome I. This ORF encodes a protein with a predicted molecular size of 192.5 kDa that shares the highest sequence similarity with the *S. cerevisiae* Sen1 protein (ScSen1p). For this reason, we named the purified protein SpSen1p (Sen1p of *S. pombe*). The *SEN1* gene belongs to the *DNA2*/*NAM7*/*UPF1* helicase family (*35*-*37*). When ScSen1p, SpSen1p, and Upf1p were aligned, the highest similarity was observed in the carboxyl terminus (Figure 4). However, 23.1% identity existed throughout the entire regions of ScSen1p and SpSen1p (data not shown), indicating that the purified enzyme is a true homologue of the Sen1 protein of *S. cerevisiae*. To confirm that the purified ATPase−helicase activity was indeed encoded by this ORF, we determined the molecular masses of tryptic peptides and examined whether they were identical to predicted tryptic peptides expected from this ORF. All nine tryptic peptides examined were found within the carboxyl-terminal half of the ORF (Figure 4). This suggested that the 95 kDa protein we purified was likely to be a proteolytic fragment (~830 amino acids) from the carboxyl terminus of the intact enzyme. Its being a helicase is in agreement with the fact that the C-terminal half of ScSen1p contains conserved helicase motifs that are required for ATP hydrolysis and unwinding activities (*18*). This suggests that the 181-kDa enzyme, similar to the 95-kDa protein in biochemical activities, is the intact size of the SpSen1p. To examine this possibility, we raised polyclonal antibodies against C-terminal region (amino acid positions 1493−1687) of SpSen1p expressed in and purified from *E. coli*. As shown in Figure 5, both the 95- and 181-kDa proteins cross-reacted with the same polyclonal antibodies specific to the C-terminus of SpSen1p. In addition, it was found by the use of western analysis that the 181-kDa polypeptide was converted spontaneously to the 95-kDa protein during early stages of purification, probably due to proteases present particularly in the fractions (data not shown). This further suggests that the 95-kDa enzyme arose by proteolysis of the

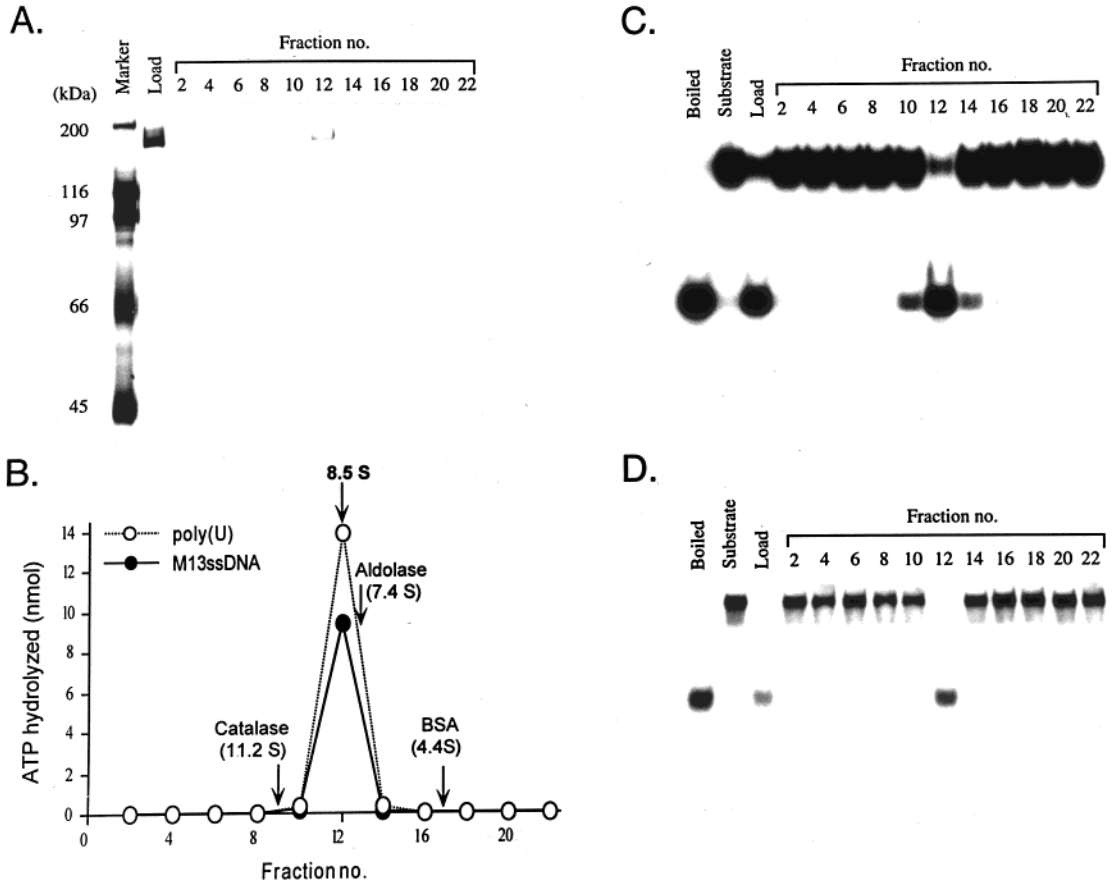

FIGURE 3: Glycerol gradient sedimentation analysis of the 181-kDa enzyme obtained from FPLC Resource S. The fractions (16 μg, 0.2 mL), which were pooled from the FPLC Resource S column and concentrated, were loaded onto a 15−35% glycerol gradient and centrifuged as described under Experimental Procedures. Fractions (0.22 mL) were collected from the bottom of the tube. Proteins were analyzed as described in Figure 2. (A) Silver-stained protein gel of the glycerol gradient fractions (20 μL). The load (pooled fractions from the FPLC Resource S column step) and glycerol gradient fractions analyzed are indicated at the top of the figure. The same size markers were used as in Figure 2. The sedimentation value of the helicase (8.5 S) was determined with reference to marker proteins, which included BSA (4.4 S), aldolase (7.4 S), and catalase (11.2 S) that were sedimented in a parallel gradient. The sedimentation profiles of the marker proteins were determined by use of the Bradford protein assay (*50*). (B) M13 sscDNA-dependent (●) and poly(U)-dependent (○) ATPase activities were measured. The ATPase activity was assayed with 2 μL of each glycerol gradient fraction in 20-μL reactions in the presence of 1.5 mM ATP as described under Experimental Procedures. (C, D) Autoradiograms of the DNA (panel C) and RNA helicase (panel D) reactions are shown. DNA and RNA helicase activities were measured in reaction mixtures (20 μL) that contained 2 μL of each glycerol gradient fraction with 20 fmol of D-STD and R-STD substrates under the conditions described in Experimental Procedures. The reaction products were resolved by electrophoresis through a 10% nondenaturing polyacrylamide gel. The boiled substrate, substrate-only, and load controls are indicated above the appropriate lanes.

181-kDa enzyme. We conclude that the enzyme we purified from *S. pombe* cells is a true homologue of *S. cerevisiae* Sen1p.

Titration and Kinetic Analysis of Displacement Reactions by SpSen1p. In the absence of NaCl, RNA substrates were more readily unwound than DNA substrates (Table 2). The addition of 25−50 mM NaCl, however, stimulated reactions containing duplex DNA more (5-fold) than reactions containing duplex RNA (2-fold), rendering the efficiency of DNA unwinding more than or at least equivalent to that of RNA unwinding (Table 2). Therefore, we decided to characterize the unwinding reactions in the presence of 50 mM NaCl hereafter.

The unwinding properties of both 95- and 181-kDa enzymes were first examined under standard assay conditions that contained 50 mM NaCl as described under Experimental Procedures. The reactions were carried out in the presence of increasing amounts of each enzyme (7−110 fmol; 1.3−20.0 ng of the 181-kDa enzyme, 0.7−10.5 ng of the 95-kDa enzyme) with standard substrates R-STD (Figure 6A, lanes 3−12) or D-STD (Figure 6B, lanes 3−12). The unwinding of R-STD substrate by the 181-kDa enzyme was more efficient (2-fold) than that by the 95-kDa enzyme at enzyme levels at which the helicase activity responded linearly to enzyme addition (Figure 6A,C). However, this difference was not reproducible with different enzyme preparations (data not shown). In contrast, the unwinding of the D-STD substrate by the two enzymes was comparable (Figure 6B,D). The amount of products formed with D-STD was more than that with R-STD substrate, especially at low enzyme levels (<28 fmol) (Figure 6C,D).

The rate of unwinding of a variety of substrates in the presence of the 181-kDa enzyme was examined. The experiments were carried out in reaction mixtures (120 μL) containing 330 fmol of SpSen1p (181-kDa enzyme) and 240 fmol of each substrate that includes R-STD, D-STD, R-74bp, and D-33bp. After varying periods of the incubation, aliquots (20 μL) were withdrawn and products formed were analyzed. As shown in Figure 7, the D-STD substrate was more rapidly unwound than the R-STD substrate and plateaued after 15

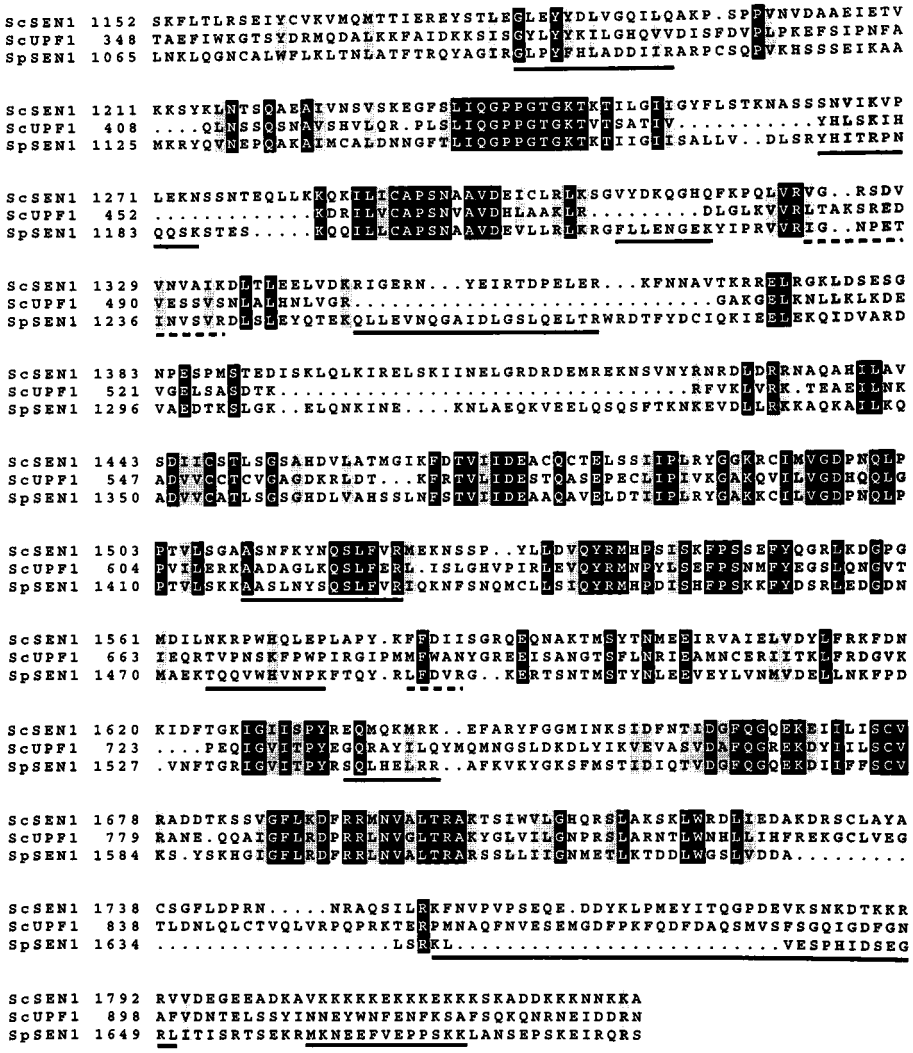

FIGURE 4: Amino acid sequence alignment between the yeast Sen1 and Upf1 proteins and the *S. pombe* Sen1 protein. The most conserved regions of the three proteins (single-letter code) were aligned to illustrate their similarities. Gaps introduced during alignment are indicated as dots. Identical amino acids are indicated in black boxes, and conserved amino acids are in shaded boxes. Amino acid sequences determined are underlined with broken lines, while tryptic peptide fragments that have the identical molecular size predicted from mass determination are underlined with solid lines. Sequence alignment was performed with the GCG program Pileup. Accession numbers of each gene from the GenBank database are as follows: M74589, *SEN1* (*S. cerevisiae*); M76659, *UPF1* (*S. cerevisiae*); Z81317, *sen1*$^+$ (*S. pombe*).

min of incubation. The efficiency of unwinding decreased substantially as the length of the duplex was increased. Although D-STD (21 bp) was efficiently unwound by SpSen1p, a slight increase in the duplex length (D-33bp) reduced the unwinding efficiency dramatically (10−30-fold). In keeping with this observation, the enzyme barely unwound a 53-bp duplex substrate (data not shown). RNA substrates were not affected as dramatically; increase in duplex length (from 21 to 74 bp) resulted in maximally 2.5-fold decrease its helicase activity (Figure 7). The rate of displacement of the RNA substrate by the 95-kDa enzyme was similar to that observed with the 181-kDa protein (data not shown).

Because the enzyme can unwind both duplex DNA and RNA substrates, we also examined whether it utilizes homologous and heterologous duplex substrates. For this purpose, we synthesized two additional duplex substrates: (i) a DNA/RNA hybrid substrate (a 28-nt ^{32}P-labeled DNA annealed to unlabeled 98-nt RNA) and (ii) a RNA/DNA hybrid substrate (a 28-nt ^{32}P-labeled RNA annealed to unlabeled 98-nt DNA). Both hybrid molecules were unwound efficiently by either the 95- or 181-kDa enzyme (data not shown). This result, together with the above, demonstrate that the two purified enzymes are strikingly similar in their enzymatic properties and that SpSen1p is capable of unwinding all duplexes encountered during its translocation, provided the duplex length is short.

Determination of Polarity of the Helicase. The directionality of a helicase is defined by its translocation direction on the enzyme-bound nucleic acid strand. For example, the directionality of a helicase is defined as a 5′ to 3′ if the helicase can unwind a substrate that has a free 5′-single-stranded region. To determine the directionality of SpSen1p, we prepared partial duplex RNA and DNA substrates with either a free 5′ tail (R-5′tail and D-5′tail) or a free 3′ tail (R-3′tail and D-3′tail), the structures of which are shown in Figure 1. Unwinding of the R-5′tail substrate was observed (Figure 8, lanes 4 and 5) with 1−3 ng of the 181-kDa enzyme, whereas unwinding of the R-3′tail substrate did not occur even at much higher enzyme levels (3−9 ng) (Figure 8, lanes 9 and 10). When the D-5′tail or the D-3′tail substrate was incubated with increasing amounts of enzyme, the D-5′tail substrate was quantitatively unwound (Figure 8, lanes

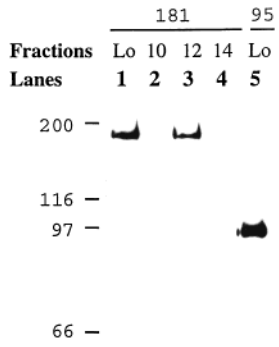

FIGURE 5: Immunological cross-reaction between the 95- and 181-kDa SpSen1p. Western immunoblotting analysis was carried out with glycerol gradient fractions of the 181-kDa (lanes 1−4) and 95-kDa (lane 5) proteins. Antisera were used at a dilution of 1:5000 in 1× TBS [40 mM Tris-HCl (pH 7.4), 7.3 mM NaCl, and 0.37 mM KCl] containing 5% nonfat milk and 0.05% Tween 20. The anti-rabbit IgG antibodies conjugated horseradish peroxidase (Amersham) were used at a dilution of 1:5000 in the same buffer described above. The detection of immobilized secondary antibodies was carried out with the ECL western blotting system (Amersham). Lane 1, load fraction (176 ng) of glycerol gradient sedimentation of the 181-kDa protein; lanes 2, 3, and 4, fractions 10, 12, and 14 (20 μL) of glycerol gradient sedimentation of the 181-kDa protein; lane 5, load fraction (300 ng) of glycerol gradient sedimentation of the 95-kDa protein.

14 and 15), but the D-3′tail substrate was not displaced at the highest enzyme level added (9 ng) (Figure 8, lane 20). This result clearly indicates that the SpSen1p helicase has a 5′ to 3′ directionality on either RNA or DNA strands. Identical observations were made with 95-kDa enzyme (data not shown).

Substrate Affinity of SpSen1p. Though the enzyme displaced either RNA or DNA duplex, the preferred substrate varied depending on the salt concentration and the length of the duplex substrate. To understand what governs unwinding efficiencies between the DNA and RNA substrates, we first determined the relative affinities of the enzyme for ssRNA and ssDNA using electrophoresis mobility shift assays and substrate competition experiments. The ability of the enzyme to form a complex with either ssDNA or ssRNA was examined with varying amounts (40, 80, and 160 fmol) of proteins (181- or 95-kDa enzymes) and a fixed level (40 fmol) of ssRNA (Figure 9A) or ssDNA (Figure 9B) substrate. As shown in Figure 9, the formation of enzyme−ssRNA and enzyme−ssDNA complexes increased linearly with the amount of protein added and was unaffected by the addition of ATP (Figure 9, both panels, compare lanes 2−4 and lanes 5−7). The complex was formed more efficiently (4−5-fold) with ssDNA (Figure 9B, lanes 2−7) than with ssRNA (Figure 9A, lanes 2−7) in the presence of the 181-kDa enzyme. Identical results were obtained with the 95-kDa enzyme, although complex formation was significantly reduced (2−3-fold) compared with the 181-kDa enzyme (Figure 9, both panels, compare lanes 8−13 and lanes 2−7). It is not clear whether the absence of the N-terminal region in the 95-kDa enzyme decreases its binding efficiency to nucleic acids. The results indicate that the enzyme either has higher affinity for ssDNA or forms a more stable complex with ssDNA, which may account for the increased unwinding of a DNA duplex under the conditions used.

The stronger affinity of the enzyme for DNA predicts that the efficiency of RNA unwinding would be affected more by the presence of ssDNA than would be the unwinding of DNA by the addition of ssRNA. To test this prediction, increasing levels (2−8-fold molar excess) of either ssDNA or ssRNA were added to reactions with a fixed amount (40 fmol) of a standard substrate (Figure 10). In the presence of a subsaturating level of enzyme (40 fmol, the 95-kDa enzyme), the unwinding reaction was more efficiently competed by ssDNA than ssRNA, as expected. Unwinding of the R-STD or D-STD substrate was more markedly reduced by the addition of ssDNA (Figure 10, both panels, lanes 7−9) than by the addition of ssRNA (Figure 10, both panels, lanes 4−6). This result strengthens the idea that the enzyme's ability to unwind duplex polynucleotides is governed in part by its affinity for nucleic acids.

Table 2: Properties of the Helicase Activities of *S. pombe* Sen1

additions or omissions	amounts added (mM)	relative activity (%)
	RNA Helicase Activity[a]	
add NaCl	0, 25, 50, 100, 200	45, 104, 100,[b] 11, 1
omit $MgCl_2$		<1
+ EDTA	1	<1
+ $MnCl_2$	1	102
+ $CaCl_2$	1	10
omit ATP		<1
+ GTP	2.5	18
+ CTP	2.5	6
+ UTP	2.5	12
+ dATP	2.5	17
+ dGTP	2.5	8
+ dCTP	2.5	4
+ dTTP	2.5	3
	DNA Helicase Activity[a]	
add NaCl	0, 25, 50, 100, 200	18, 98, 100,[c] 13, 6
omit $MgCl_2$		<1
+ EDTA	1	<1
+ $MnCl_2$	1	91
+ $CaCl_2$	1	12
omit ATP		<1
+ GTP	2.5	37
+ CTP	2.5	11
+ UTP	2.5	27
+ dATP	2.5	73
+ dGTP	2.5	30
+ dCTP	2.5	4
+ dTTP	2.5	1

[a] The complete reaction contained 181-kDa SpSen1p (27.5 fmol) in the standard reaction mixture as described under Experimental Procedures. All reactions above contained 50 mM NaCl in the reaction mixtures except the salt titration experiment as indicated. [b] Displacement of 19.0 fmol of RNA substrate is equivalent to 100%. [c] Displacement of 27.0 fmol of DNA substrate is equivalent to 100%.

Requirements for the Unwinding Reactions of the SpSen1p Helicase. Both the RNA and DNA unwinding activities of the 181-kDa SpSen1p were dependent on the presence of ATP (Figure 8, lanes 2 and 12; Table 2). Addition of EDTA (1 mM) inactivated the unwinding reaction completely, indicating that a divalent cation such as $MgCl_2$ is essential (Table 2). Both RNA and DNA helicase activities were poorly active (10−12%) when $CaCl_2$ was used in place of $MgCl_2$. However, $MnCl_2$ substituted efficiently (91−102%) for $MgCl_2$ in the unwinding of either RNA or DNA (Table 2). In the absence of NaCl, the standard DNA substrate was less efficiently unwound (4.9 fmol, 18% of 27 fmol unwound) than the standard RNA substrate (8.6 fmol, 45% of 19 fmol unwound) (Table 2). The addition of low salt concentrations (25−50 mM) increased unwinding of both

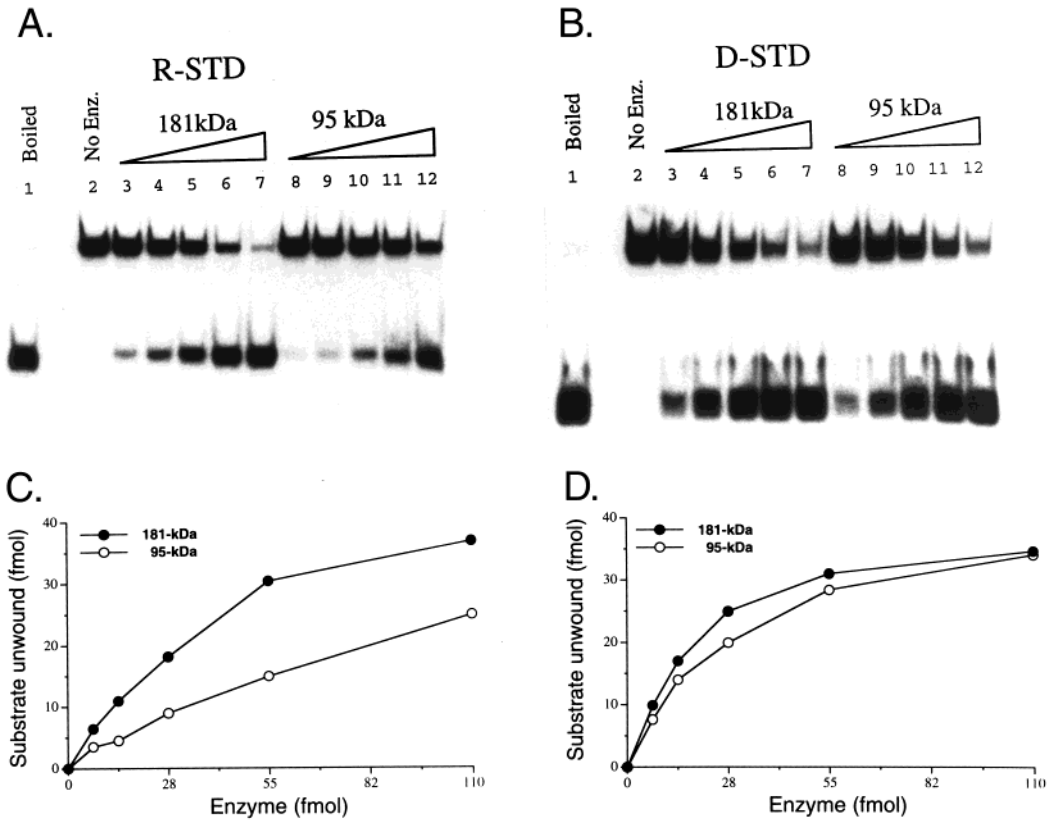

FIGURE 6: Effects of increasing amounts of enzyme on the unwinding of RNA and DNA substrates. (A, B) Unwinding activities of the 95-kDa and 181-kDa enzymes were measured in standard reaction mixtures (20 μL) that contained increasing amounts of the enzyme with 40 fmol of R-STD (panel A) and D-STD (panel B). The amount of enzyme in each lane was as follows; 7 fmol, lanes 3 and 8; 14 fmol, lanes 4 and 9; 27.5 fmol, lanes 5 and 10; 55 fmol, lanes 6 and 11; 110 fmol, lanes 7 and 12. Boiled substrate (lane 1) and substrate only (lane 2) controls are also denoted. (C, D) Quantitation of substrate unwound in panels A and B, respectively. Symbols for each enzyme are as indicated in the graph.

RNA and DNA duplex substrates (Table 2); low levels of NaCl to the reaction stimulated the unwinding of the DNA substrates more than the RNA substrates (2-fold) (Table 2). Both RNA and DNA unwinding were significantly inhibited by higher salt concentrations (<10% at 200 mM NaCl) (Table 2).

At high concentrations (2.5 mM) of nucleoside triphosphates, ATP, GTP, CTP, UTP, dATP, and dGTP, the enzyme catalyzed the unwinding of significant levels (>5%) of the input RNA substrate (Table 2). DNA unwinding was supported similarly by the same nucleoside triphosphates, although the overall unwinding efficiency was greater (2−4-fold) (Table 2). At lower NTP concentrations (0.5 mM), ATP, GTP, and dATP supported DNA unwinding efficiently but hardly supported the unwinding of RNA (data not shown), indicating that K_m of the nucleoside triphosphates is higher for RNA unwinding than DNA unwinding.

Effects of Various Polynucleotides on ATP Hydrolysis and Characterization of the ATPase Activity of SpSen1p. Because both ssDNA and ssRNA supported ATP hydrolysis by 181-kDa SpSen1p, we first determined the requirements of the ATPase in the presence of saturating amounts (50 ng) of either poly(U) or M13 sscDNA in the standard reaction mixture as described under Experimental Procedures. Under these reaction conditions, ATP hydrolysis was slightly more efficient (about 1.2-fold) in the presence of poly(U) than with M13 ssDNA (Table 3). The addition of NaCl (25−200 mM) affected the poly(U)-dependent and M13 sscDNA-dependent ATPase activities similarly (Table 3). Both RNA- and DNA-dependent ATPase activities were slightly stimulated (up to 130%) by the addition of 25−50 mM NaCl. Higher levels of NaCl were inhibitory (Table 3). The enzyme required $MgCl_2$ for ATP hydrolysis, and $CaCl_2$ and $MnCl_2$ substituted partially (11−17% and 54−62%, respectively) for $MgCl_2$ (Table 3).

We also investigated the effects of various polynucleotides on the ATPase activity of SpSen1p. For this purpose, reactions were carried out in the presence of the increasing amounts of various polynucleotides with 27.5 fmol of purified 181-kDa enzyme (Table 3). Polyribonucleotides poly(U), poly(A), and poly(C) supported ATP hydrolysis, whereas poly(G) did not (Table 3). M13 sscDNA and RF1 also stimulated ATPase activity, but to a lesser extent than did poly(U) at a high concentration (5 ng) (Table 3). At low concentrations (<1 ng/reaction), M13 sscDNA or RF1 stimulated ATP hydrolysis more efficiently (> 2-fold) than did poly(U) (data not shown). In contrast to observation with native DNA, homopolymeric DNAs such as poly(dT) and poly(dA) failed to support the ATPase activity of the 181-kDa enzyme. This suggests that SpSen1p may require secondary structures or duplex DNA for its ATPase and unwinding activities. We also tested whether yeast tRNA (native and denatured) served as a cofactor in the ATP hydrolysis reaction in place of synthetic homopolymeric RNA. Surprisingly, yeast tRNA was inefficient in supporting ATP hydrolysis (Table 3). At the lowest level of tRNA (1 ng), the enzyme was virtually inactive, while the 98-mer ssRNA, which is similar to tRNA in size, was a moderate

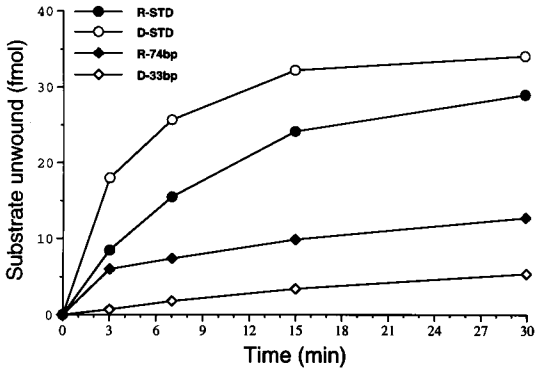

FIGURE 7: Kinetic analyses of the unwinding activity of the helicase. Kinetic experiments were carried out to measure the rate of unwinding as described under Experimental Procedures. The reaction mixtures (120 μL) contained 330 fmol of 181-kDa enzyme and 240 fmol of R-STD (21 bp) (●), R-74bp (74 bp) (◆), D-STD (21 bp) (○), and D-33 bp (33 bp) (◇) substrates; the duplex length of each substrate is denoted in parentheses. Aliquots (20 μL) were withdrawn after 3, 7, 15, and 30 min of incubation, and reactions were stopped and subjected to electrophoresis on a 10% nondenaturing polyacrylamide gel.

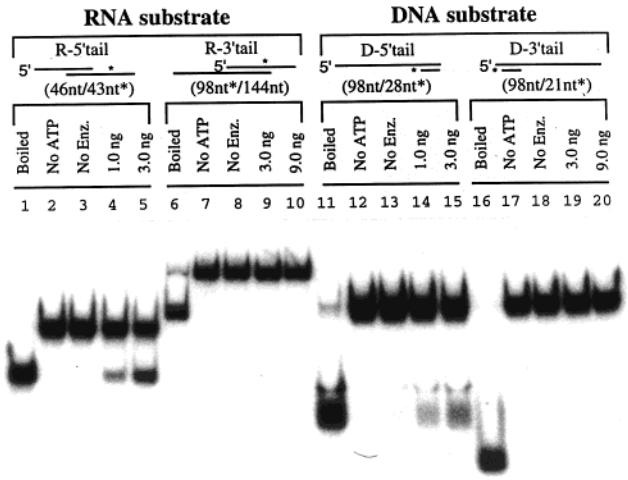

FIGURE 8: Translocation of the helicase in the 5′ to 3′ direction. The schematic structures of RNA (R-5′tail, R-3′tail) and DNA (D-3′tail, D-5′tail) substrates used to determine the directionality of the helicase are shown at top of the figure. Asterisks indicate radioisotope-labeled strands; DNAs were labeled at their 3′-ends, and RNAs were internally labeled during transcription. The unwinding direction was determined with 20 fmol of substrate and the indicated amounts of protein under the standard reaction conditions described in Experimental Procedures. Substrate only (No Enz.), omission (No ATP), and boiled controls are indicated.

effector of ATP hydrolysis (Table 3). At much higher tRNA levels (25 ng), the level of ATP hydrolyzed was comparable to that obtained with 1 ng of ssRNA of similar size (data not shown). In conclusion, the finding that both DNA and RNA support ATP hydrolysis suggests that SpSen1p probably unwinds both DNA and RNA duplex structure in vivo.

DISCUSSION

We have isolated two biochemically related helicase activities from extracts of *S. pombe* cells that unwind both DNA and RNA duplexes and translocate in the 5′ to 3′ direction. Amino acid sequences of tryptic peptides derived from the purified enzyme (95 kDa), which revealed that it is encoded by the *S. pombe* homologue of yeast *SEN1*. The discrepancy between the size of the purified enzyme and the

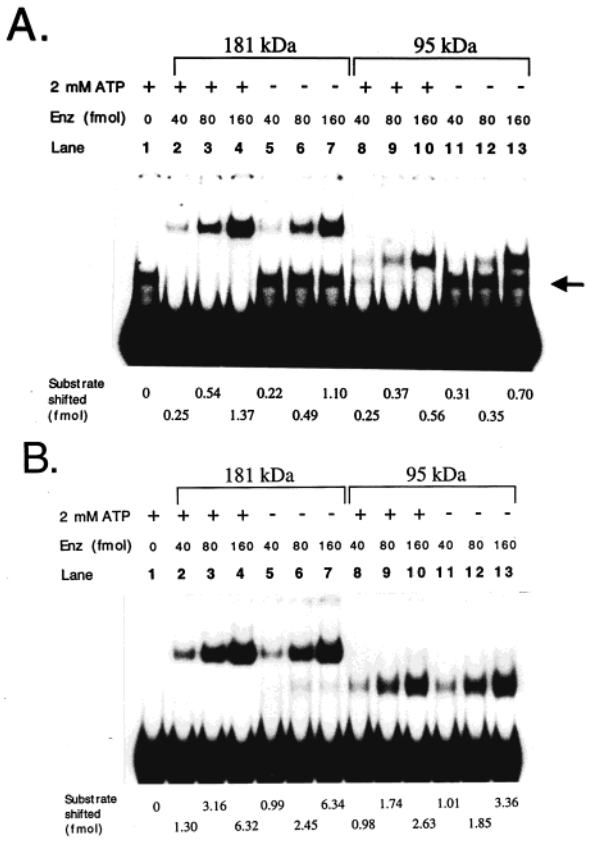

FIGURE 9: Determination of the enzyme's affinity for ssDNA and ssRNA. Substrate−enzyme complexes were generated under the reaction conditions described in Experimental Procedures. The reaction mixtures (20 μL) contained increasing amounts (40, 80, and 160 fmol) of enzyme with 40 fmol of internally labeled ssRNA (98-mer) (panel A) or 5′-labeled ssDNA (98-mer) (panel B) in the presence or absence of 2 mM ATP. The arrow indicates an RNA species formed due to the secondary structure of ssRNA, which disappeared on the addition of enzyme and ATP (lanes 2−4 and 8−10). The resulting nucleoprotein complexes were analyzed as described under Experimental Procedures. Amounts of complex formed are indicated at the bottom of the figure.

molecular size predicted from the *sen1*$^+$ ORF (1688 amino acids, 192.5 kDa) was resolved by our isolation of a larger polypeptide (181 kDa) with biochemical properties strikingly similar to those of the 95-kDa enzyme. Both enzymes unwound DNA and RNA duplex molecules, translocated in the 5′ to 3′ direction, and shared strikingly similar biochemical properties with regard to polynucleotide effect, hydrolysis of nucleoside triphosphates, and salt sensitivity. More conclusively, both the purified 95-kDa and 181-kDa polypeptides were detected by the same polyclonal antibody raised against a truncated polypeptide containing the carboxyl-terminal 195 amino acids (Figure 5). On the basis of these results, we conclude that the purified enzyme is encoded by the *sen1*$^+$ gene of *S. pombe*.

Surprisingly, the determination of enzymatic properties of the two enzymes purified revealed that the loss of the N-terminal half of SpSen1p did not compromise the helicase and nucleic acid-dependent ATPase activities. Since the carboxy-terminal 1214 amino acids of ScSen1p that contain all of the helicase motifs are essential for cell's growth, whereas the amino-terminal 898 amino acids are dispensable (*18*), unwinding and ATP hydrolysis activities of the enzyme are believed to be essential for biological functions in vivo

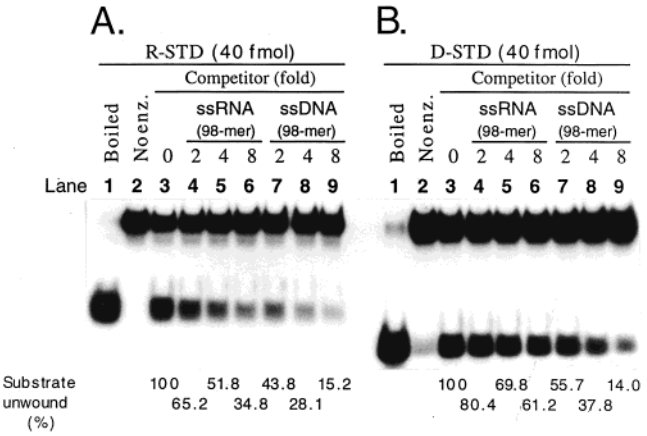

FIGURE 10: Inhibitions of competitors on the unwinding of RNA and DNA substrates. Unwinding reactions were performed with R-STD (panel A) and D-STD (panel B) in the presence of the indicated amounts of unlabeled 98-mer ssRNA or unlabeled 98-mer ssDNA as competitors in the standard reaction mixture, which contained 40 fmol of the 95-kDa enzyme. The amount of each substrate unwound in the presence of varying concentrations of competitor is indicated at the bottom of the figure. The amount of R-STD and D-STD unwound (15.7 and 9.4 fmol, respectively) in the absence of competitor was equivalent to 100%.

Table 3: Properties of the ATPase Activities of *S. pombe* Sen1[a]

additions or omissions	amounts added	relative activity (%)
	Poly(U)-Dependent ATPase	
add NaCl	0, 25, 50, 100, 200 mM	84, 90, 100,[b] 68, 3
omit $MgCl_2$		<1
+ EDTA	1 mM	<1
+ $MnCl_2$	1 mM	62
+ $CaCl_2$	1 mM	11
	M13 ssDNA-Dependent ATPase	
add NaCl	0, 25, 50, 100, 200 mM	73, 80, 87, 48, 1
omit $MgCl_2$		<1
+ EDTA	1 mM	<1
+ $MnCl_2$	1 mM	54
+ $CaCl_2$	1 mM	17
	Other Polynucleotides	
omit polynucleotide		<1
+ poly(A)	1, 5 ng	10, 34
+ poly(C)	1, 5 ng	10, 30
+ poly(G), (dT), or (dA)	1, 5 ng	1, <5
+ M13 ssDNA	1, 5 ng	58, 70
+ M13 RFI DNA	1, 5 ng	73, 80
+ ssDNA (98-mer)	1, 5 ng	46, 55
+ ssRNA (98-mer)	1, 5 ng	8, 16
+ yeast tRNA	1, 5 ng	1, 2
+ yeast tRNA, boiled	1, 5 ng	1, 2

[a] The complete reaction contained the 181-kDa SpSen1p (27.5 fmol) in the standard reaction mixture that included 50 mM NaCl as described under Experimental Procedures. The concentrations of NaCl were varied as indicated in the salt titration experiment only. [b] The hydrolysis of 1.69 nmol of ATP is equivalent to 100%.

of SpSen1p. This fact, however, does not exclude the possibility that the N-terminal region of Sen1 may have a potential role(s) in vivo to regulate the enzymatic activities. For example, this region may act as a regulatory domain to affect biochemical activities of Sen1 in vivo in a way that cannot be detected in vitro with the purified enzyme alone or to mediate protein−protein interactions between Sen1 and other unidentified protein(s). In other words, this function may be required for an optimized action in vivo of Sen1 in conjunction with other unknown protein(s). Alternatively, this region may have a role specific for a subset only among many RNA transactions requiring Sen1, the defect of which is not deleterious to the cell's growth. These possibilities are highly speculative and, thus, need to be explored in the future.

The enzyme's ability to function as an RNA and DNA helicase in the 5′ to 3′ direction limits the number of potential biochemical homologues among known eukaryotic helicases. Only two eukaryotic helicases have been reported that possess both DNA and RNA unwinding activities and translocate in the same direction as the purified enzyme. These are human DNA helicase IV (HDH IV) (*38*), encoded by the nucleolin gene (*39*), and *S. cerevisiae* Upf1p (*24*), which is involved in nonsense-mediated mRNA decay (*35*, *40*). Thus, these two helicases share some fundamental properties with our *S. pombe* enzyme. In other respects, however, they differ from the *S. pombe* helicase. For example, HDH IV is not able to utilize nucleoside triphosphates other than ATP and dATP, unlike the *S. pombe* protein. Although Upf1p (109 kDa) is similar in size to the purified enzyme (95 kDa), other biochemical properties differ between the two proteins. For example, the magnitude of the ATP hydrolysis rate differs greatly between the two proteins (30 ATP s^{-1} $enzyme^{-1}$ for the *S. pombe* helicase vs 1 ATP s^{-1} $enzyme^{-1}$ for Upf1p). ATP hydrolysis by Upf1p was inefficient in the presence of poly(A), whereas the *S. pombe* enzyme hydrolyzed ATP most efficiently in the presence of poly(A) (Table 3). Another notable difference is that complex formation between Upf1p and ssRNA is reduced markedly in the presence of hydrolyzable ATP, whereas *S. pombe* helicase complex formation was not affected by the presence of ATP (Figure 9A).

It was shown recently that Sen1 affects the biosynthesis and/or processing of diverse RNAs including tRNAs, rRNAs, and small nuclear and nucleolar RNAs. Thus, a mutation in the SEN1 gene results in pleiotropic defects in RNA metabolism (*29*). In the temperature-sensitive *SEN1* mutant (*sen1-1*), the steady-state levels of these RNAs were significantly altered in abundance (decreased or increased) upon growth at the nonpermissive temperature (*29*). Recently, another allele of *SEN1* altered the expression of a chimeric reporter gene containing an exogenously inserted cis-acting element (*28*), indicating that Sen1 also affects mRNA synthesis. The primary effect of the insertion is a 20-fold decrease in pre-mRNA abundance accompanied by the appearance of 3′-truncated transcripts. However, a point mutation at a conserved residue near the predicted ATP binding motif of *SEN1* relieved the negative effects of the cis element (*28*). In summary, pleiotropic defects associated with *SEN1* mutations are categorized into three groups: (i) increased levels of precursor tRNA and rRNA (*17*, *29*), (ii) decreased levels of small nucleolar RNAs (snoRNAs) with increased levels of truncated snoRNAs in some cases (*29*), and (iii) increased pre-mRNA levels (*28*).

At present, it is difficult to present a single hypothesis that accommodates all of these complicated and apparently unrelated phenotypes. A common denominator for all of these phenomena could be defects in RNA processing that occur either directly or indirectly. As a molecular mechanism to account for defective RNA processing, it was suggested that *SEN1* may facilitate appropriate nucleolytic cleavages for the processing of target RNAs (*29*). In support of this, it

was recently shown that a temperature-sensitive mutation (*sen1-1*) of the *SEN1* gene of *S. cerevisiae* resulted in defective maturation and reduced stability of termini of snoRNAs (*31*). In this study, the processing of snR13, a snoRNA, was closely examined. When *sen1-1* mutant cells were shifted to the nonpermissive temperature, newly synthesized snR13F (the mature form of snR13) was markedly decreased, whereas snR13R (3′ extended form) and snR13T (5′ truncated form) were increased (*31*). Considering that snoRNAs are required for processing and posttranscriptional modification of rRNA (*41*−*43*), this result suggests that defective processing of rRNA occurs as a secondary consequence of perturbations in the synthesis of snoRNAs in *sen1-1* mutant cells.

The fact that SpSen1p is an RNA helicase that translocates in the 5′ to 3′ direction (Figure 8) suggests that the enzyme may act in the processing of precursor RNAs. While Sen1p translocates along the growing RNA chain as transcription proceeds in a coupled fashion, it may recruit or activate a processing enzyme in response to a molecular signal, such as a specific cis element or structure in the nascent RNA. This in turn would allow for the processing of the RNA transcripts. The mutation in the *sen1-1* allele (*29*) may hamper the enzyme's ability either to interact with an appropriate processing enzyme or to translocate along RNA transcripts, resulting in faulty processing that increases the levels of unprocessed RNA. In favor of this hypothesis, several RNA helicases such as RlhB and Suv3 are known to stably associate with endo- and/or exonucleases (*44*, *45*). However, we failed to detect any nucleolytic activity associated with our final preparations of SpSen1p (data not shown), suggesting that a processing enzyme, if any, is not stably complexed with SpSen1p. It is possible that the enzyme may contain intrinsic nucleolytic activity that acts on a specific sequence or structure within the target RNAs that was not present in the substrates used in this study. The requirement for a specific sequence or structure is consistent with the observations that (i) a certain class of RNA coimmunoprecipitates with ScSen1p and polyclonal antibodies specific to this enzyme (*29*) and (ii) a specific sequence element represses gene expression only in the presence of wild-type ScSen1p (*28*).

The tRNA biogenesis appears more complicated than the processing of snoRNA by Sen1p. The primary defect responsible for the accumulation of intron-containing pre-tRNAs in cells carrying the *sen1-1* mutation is still unknown, since the accumulation of tRNA precursors observed in *sen1-1* cells does not correlate with growth temperature. The mutation caused a 10-fold increase in the accumulation of pre-tRNAs at both permissive and nonpermissive temperature. What is still not understood is that a 90% reduction in the in vitro activity of tRNA-splicing endonuclease complex was observed in the *sen1-1* cells, although it was demonstrated that the Sen1 protein is not a subunit of the complex endonuclease (*20*).

Despite the lack of evidence for direct involvement of Sen1p in tRNA splicing, it may be that Sen1 affects the processing of both snoRNA and tRNA through a common mode of action. The predicted secondary structure of snR13 shares features strikingly similar to tRNA (*31*). They are both short RNAs with four stem and loop structures, although modified bases have not been detected in the snR13, except for the trimethylguanosine at the 5′ end (*31*). Sen1p might be required for the endonucleolytic cleavage that is required for the maturation of these two RNA species. For example, it could form a complex that functions as a landing pad for recruiting the catalytic endonuclease. If ATP hydrolysis and unwinding activities are essential, the unwinding activity might be used to alter transiently a stable secondary structure of the precursor RNA, facilitating subsequent enzymatic action such as cleavage by the endonuclease. Since the carboxyl-terminal region of ScSen1p that contains all of the essential helicase motifs is required for the cell's viability (*18*), it is possible that the helicase activity is an essential activity for RNA processing. Genetic and biochemical analyses of mutants defective in ATP hydrolysis are necessary to address whether the biochemical activities discovered in this study are essential for RNA processing. The two mechanisms described above would enhance the overall efficiency and/or fidelity of RNA processing in vivo. This hypothesis is consistent with the observation that the ScSen1p is not a catalytic subunit (*20*) but plays an indirect role in the removal of tRNA introns (*18*, *25*). Therefore, it would be interesting to test whether in vitro Sen1p enhances the overall efficiency of tRNA splicing by the enzymes that support tRNA maturation.

Although the mechanisms discussed above account for the increased levels in unprocessed RNAs, they fail to explain how the same mutation leads to a decrease in the levels of certain RNA species. This observation suggests that Sen1p may have a positive role in RNA transcription as described below. Although SpSen1p's ability to unwind duplex RNA fits with the idea that it is required for the biosynthesis of a wide range of RNA species, the role of the duplex DNA and DNA/RNA hybrid unwinding activities is not clear at present. The DNA unwinding activity of SpSen1p was at least comparable to or more potent than its RNA unwinding activity with short duplex substrates. Therefore, the enzyme may also play a role in biological transactions that require unwinding of DNA or DNA/RNA hybrids of limited lengths. If the *sen1-1* mutation reduces the expression of specific genes (for example, those encoding subunits of the tetrameric tRNA splicing endonuclease), it would result in a phenotype identical to that originally reported and could account for the following puzzling results (*17*): (i) the tRNA-splicing endonuclease activity was significantly reduced, (ii) the activity of the partial purified endonuclease from temperature-sensitive *sen1-1* mutant cells was not affected by incubation temperature, and (iii) extracts prepared from *sen1-1* mutant cells failed to complement *sen2-1* mutant extracts in tRNA cleavage. One possible explanation is that the defect caused by the *sen1-1* mutation is established prior to protein synthesis. This is in keeping with recent observations that the *sen1-1* mutation affected RNA biosynthesis (*29*). The participation of an enzyme having both DNA and RNA helicase activity in transcription is not unprecedented. The MLE protein of *Drosophila melanogaster*, RNA helicase A from HeLa cells, and nuclear DNA helicase II share substantial amino acid homologies (*46*−*48*) and unwind both RNA and DNA duplexes (*14*, *49*). The MLE protein functions in dosage compensation by elevating the transcription of many genes on a single copy of the X chromosome in a male fruit fly (*47*). Human RNA helicase A was recently reported to be involved in activated RNA transcription by

mediating the association of coactivator CBP with RNA polymerase II, which is required to stimulate transcription of certain signal-dependent genes (*16*).

The biochemical properties defined here for SpSen1p permit us to begin to understand its action as a key player in a variety of RNA metabolic events. We expect that many of the unresolved issues discussed here will be clarified by extending the biochemical information derived from our present study to a more focused genetic approach.

ACKNOWLEDGMENT

We express special thanks to Drs. H. Erdjument-Bromage and P. Tempst of the Microchemistry Laboratory of Sloan-Kettering Institute (New York) for the protein sequencing work and mass determination of the tryptic peptides of SpSen1p and to Dr. J. Hurwitz for critical reading of the manuscript.

REFERENCES

1. Matson, S. W., and Kaiser-Rogers, K. (1990) *Annu. Rev. Biochem. 59*, 289−329.
2. Thommes, P., and Hubscher, U. (1992) *Chromosoma 101*, 467−473.
3. Matson, S. W., Bean, D. W., and George, J. W. (1994) *BioEssays 16*, 13−22.
4. Lohman, T. M., and Bjornson, K. P. (1996) *Annu. Rev. Biochem. 65*, 169−214.
5. Tuteja, N., and Tuteja, R. (1996) *Nat. Genet. 13*, 11−12.
6. West, S. C. (1996) *Cell 86*, 177−180.
7. Gorbalenya, A. E., Koonin, E. V., Donchenko, A. P., and Blinov, V. M. (1989) *Nucleic Acids Res. 17*, 4713−4730.
8. Goffeau, A., Barrell, B. G., Bussey, H., Davis, R. W., Dujon, B., Feldmann, H., Galibert, F., Hoheisel, J. D., Jacq, C., Johnston, M., Louis, E. J., Mewes, H. W., Murakami, Y., Philippsen, P., Tettelin, H., and Oliver, S. G. (1996) *Science 274*, 563−567.
9. Foury, F., and Lahaye, A. (1987) *EMBO J. 6*, 1441−1449.
10. Schulz, V. P., and Zakian, V. A. (1994) *Cell 76*, 145−155.
11. Ellis, N. A., Groden, J., Ye, T. Z., Straughen, J., Lennon, D. J., Ciocci, S., Proytcheva, M., and German, J. (1995) *Cell 83*, 655−666.
12. Yu, C. E., Oshima, J., Fu, Y. H., Wijsman, E. M., Hisama, F., Alisch, R., Matthews, S., Nakura, J., Miki, T., Ouais, S., Martin, G. M., Mulligan, J., and Schellenberg, G. D. (1996) *Science 272*, 258−262.
13. Lee, C. G., and Hurwitz, J. (1992) *J. Biol. Chem. 267*, 4398−4407.
14. Lee, C. G., Chang, K. A., Kuroda, M. I., and Hurwitz, J. (1997) *EMBO J. 16*, 2671−2681.
15. Tang, H., Gaietta, G. M., Fischer, W. H., Ellisman, M. H., and Wong-Staal, F. (1997) *Science 276*, 1412−1415.
16. Nakajima, T., Uchida, C., Anderson, S. F., Lee, C. G., Hurwitz, J., Parvin, J. D., and Montminy, M. (1997) *Cell 90*, 1107−1112.
17. Winey, M., and Culbertson, M. R. (1988) *Genetics 118*, 609−617.
18. DeMarini, D. J., Winey, M., Ursic, D., Webb, F., and Culbertson, M. R. (1992) *Mol. Cell. Biol. 12*, 2154−2164.
19. Ho, C. K., Rauhut, R., Vijayraghavan, U., and Abelson, J. (1990) *EMBO J. 9*, 1245−1252.
20. Trotta, C. R., Miao, F., Arn, E. A., Stevens, S. W., Ho, C. K., Rauhut, R., and Abelson, J. (1997) *Cell 89*, 849−858.
21. Greer, C. L., Peebles, C. L., Gegenheimer, P., and Abelson, J. (1983) *Cell 32*, 539−536.
22. Phizicky, E. M., Schwartz, R. C., Knapp, G., and Abelson, J. (1986) *J. Biol. Chem. 261*, 2978−2988.
23. MaCraith, S. M., and Phizicky, E. M. (1991) *J. Biol. Chem. 266*, 11986−11992.
24. Czaplinski, K., Weng, Y., Hagan, K. W., and Peltz, S. W. (1995) *RNA 1*, 610−623.
25. Ursic, D., DeMarini, D, J., and Culbertson, M. R. (1995) *Mol. Gen. Genet. 249*, 571−584.
26. Clark, M. W., Yip, M. L., Campbell, J., and Abelson, J. (1990) *J. Cell Biol. 111*, 1741−1751.
27. Tollervey, D., Lehtonen, H., Carmo-Fonseca, M., and Hurt, E. C. (1991) *EMBO J. 10*, 573−583.
28. Steinmetz, E. J., and Brow, D. A. (1996) *Mol. Cell. Biol. 16*, 6993−7003.
29. Ursic, D., Himmel, K. L., Gurley, K. A., Webb, F., and Culbertson, M. R. (1997) *Nucleic Acids Res. 25*, 4778−4785.
30. Page, B. D., and Snyder, M. (1992) *Genes Dev. 6*, 1414−1429.
31. Rasmussen, T. P., and Culbertson, M. R. (1998) *Mol. Cell. Biol. 18*, 6885−6896.
32. Messing, J. (1983) *Methods Enzymol. 101*, 20−78.
33. Sambrook, J., Fritsch, E. F., and Maniatis, T. (1989) *Molecular Cloning: A Laboratory Manual*, 2nd ed., Cold Spring Harbor Laboratory, Cold Spring Harbor, NY.
34. Park, J. S, Choi, E., Lee, S.-H., Lee, C., and Seo, Y.-S. (1997) *J. Biol. Chem. 272*, 18910−18919.
35. Leeds, P., Wood, J. M., Lee, B. S., and Culbertson, M. R. (1992) *Mol. Cell. Biol. 12*, 2165−2177.
36. Altamura, N., Groudinsky, O., Dujardin, G., and Slonimski, P. P. (1992) *J. Mol. Biol. 224*, 575−587.
37. Koonin, E. V. (1992) *Trends Biochem. Sci. 17*, 495−497.
38. Tuteja, N., Rahman, K., Tuteja, R., and Falaschi, A. (1991) *Nucleic Acids Res. 19*, 3613−3618.
39. Tuteja, N., Huang, N. W., Skopac, D., Tuteja, R., Hrvatic, S., Zhang, J., Pongor, S., Joseph, G., Faucher, C., Amalric, F., and Falashi, A. (1995) *Gene 160*, 143−148.
40. Leeds, P., Peltz, S. W., Jacobson, A., and Culbertson, M. R. (1991) *Genes Dev. 5*, 2303−2314.
41. Mattaj, I. W., Tollervey, D., and Seraphin, B. (1993) *FASEB J. 7*, 47−53.
42. Maxwell, E. S., and Fournier, M. J. (1995) *Annu. Rev. Biochem. 64*, 897−934.
43. Tollervey, D., and Kiss, T. (1997) *Curr. Opin. Cell Biol. 9*, 337−342.
44. Margossian, S. P., Li, H., Zassenhaus, H. P., and Butow, R. A. (1996) *Cell 84*, 199−209.
45. Py, B., Higgins, C. F., Krisch, H. M., and Carpousis, A. J. (1996) *Nature 381*, 169−172.
46. Kuroda, M. I., Kernan, M. J., Kreber, R., Ganetzky, B., and Baker, B. S. (1991) *Cell 66*, 935−947.
47. Lee, C. G., and Hurwitz, J. (1993) *J. Biol. Chem. 268*, 16822−16830.
48. Zhang, S., Maacke, H., and Grosse, F. (1995) *J. Biol. Chem. 270*, 16422−16427.
49. Zhang, S., and Grosse, F. (1994) *Biochemistry 33*, 3906−3912.
50. Bradford, M. M. (1976) *Anal. Biochem. 72*, 248−254.

BI991470C